

Dibenzo[*f,h*]thieno[3,4-*b*] quinoxaline-Based Small Molecules for Efficient Bulk-Heterojunction Solar Cells

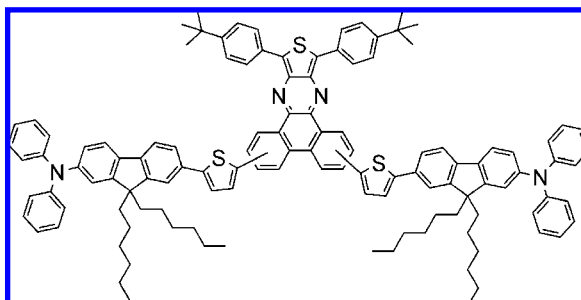
Marappan Velusamy,[†] Jen-Hsien Huang,[‡] Ying-Chan Hsu,[†] Hsien-Hsin Chou,[†]
Kuo-Chuan Ho,[‡] Pei-Lun Wu,[†] Wei-Hau Chang,[†] Jiann T. Lin,^{*,†} and
Chih-Wei Chu^{*,§}

*Institute of Chemistry and Research Center for Applied Sciences,
Academia Sinica, Nankang, Taiwan, and Department of Chemical Engineering,
National Taiwan University, Taiwan*

jtlin@chem.sinica.edu.tw; gchu@gate.sinica.edu.tw

Received August 27, 2009

ABSTRACT



Two isomeric compounds (1 and 2) containing a dibenzo[*f,h*]thieno[3,4-*b*]quinoxaline core and two peripheral arylamines were synthesized. Solution-processed bulk heterojunction (BHJ) solar cells based on these sensitizers and [6,6]-phenyl-C61-butyric acid methyl ester (PCBM) are reported. The cell fabricated from 1/67 wt % of PCBM exhibited a high power conversion efficiency of 1.70% and an external quantum yield of 55%. The film of the cell was found to have balanced electron and hole mobility and good film morphology.

Organic solar cells have been intensely explored in the past decade because of the increasing demand of sustainable and renewable energy supply arising from rapid depletion of fossil fuels and disastrous environmental problems accompanying the combustion of these fuels.¹ Among these, dye-sensitized solar cells (DSSCs) have attracted considerable interest, and an efficiency record of ~11% has been

achieved with ruthenium-based sensitizers.² Since the seminal report of Tang,³ organic photovoltaic (OPV) cells have also made significant progress, and high efficiencies at 6% and 6.7% have been reported for single⁴ and tandem⁵ cells, respectively. Organic semiconductors are attractive because of their low cost, easy manufacture of thin film by vacuum deposition, solution cast, and printing technologies. Conju-

[†] Institute of Chemistry, Academia Sinica.

[‡] Department of Chemical Engineering, National Taiwan University.

[§] Research Center for Applied Sciences, Academia Sinica.

(1) For recent reviews, see: (a) Grätzel, M. *Inorg. Chem.* **2005**, *44*, 6841. (b) Durrant, J. R.; Haque, S. A.; Palomares, E. *Chem. Commun.* **2006**, 3279. (c) Günes, S.; Neugebauer, H.; Sariciftci, N. S. *Chem. Rev.* **2007**, *107*, 1324. (d) Bundgaard, E.; Krebs, F. C. *Sol. Energy Mater. Sol. Cells* **2007**, *91*, 954. (e) Thompson, B. C.; Fréchet, J. M. J. *Angew. Chem., Int. Ed.* **2008**, *47*, 58. (f) Mishra, A.; Fisher, M. K. R.; Buerle, P. *Angew. Chem., Int. Ed.* **2009**, *48*, 2474.

(2) (a) Nazeeruddin, M. K.; DeAngelis, F.; Fantacci, S.; Selloni, A.; Viscardi, G.; Liska, P.; Ito, S.; Takeru, B.; Grätzel, M. *J. Am. Chem. Soc.* **2005**, *127*, 16835. (b) Chiba, Y.; Islam, A.; Watanabe, Y.; Komiyama, R.; Koide, N.; Han, L. *Jpn. J. Appl. Phys., Part 2* **2006**, *45*, L638. (c) Gao, F.; Wang, Y.; Zhang, J.; Shi, D.; Wang, M.; Humphrey-Baker, R.; Wang, P.; Zakeeruddin, S. M.; Grätzel, M. *Chem. Commun.* **2008**, 2629.

(3) Tang, C. W. *Appl. Phys. Lett.* **1986**, *48*, 183.

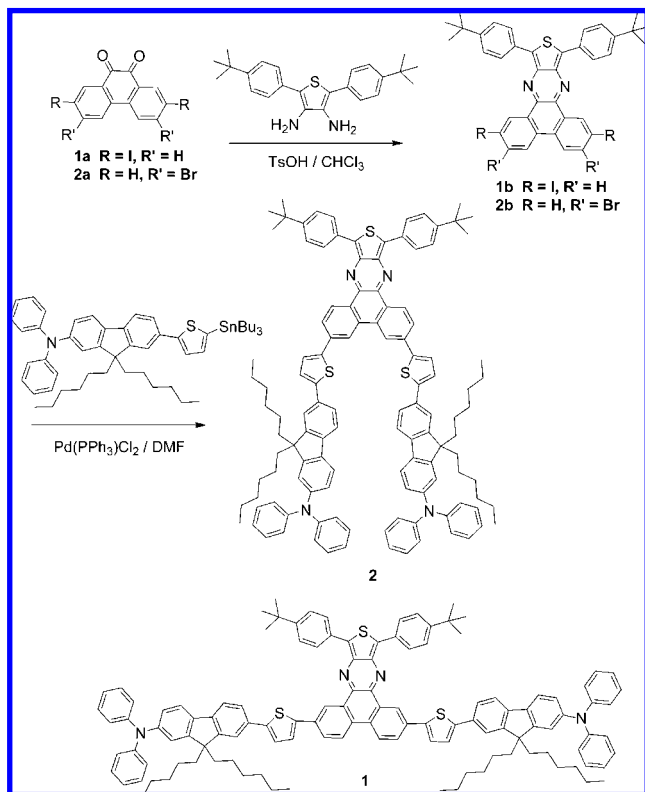
(4) Park, S. H.; Roy, A.; Beaupré, S.; Cho, S.; Coates, N.; Moon, J. S.; Moses, D.; Leclerc, M.; Lee, K.; Heeger, A. *J. Nat. Photonics* **2009**, *3*, 297.

(5) Kim, J. Y.; Lee, K.; Coates, N. E.; Moses, D.; Nguyen, T.-O.; Dante, M.; Heeger, A. *J. Science* **2007**, *317*, 222.

gated polymers have been widely used in OPV devices, with either heterojunction (HJ) or bulk heterojunction (BHJ) architecture, via solution cast. BHJ cells normally have better energy conversion efficiencies than layered HJ cells because of their limited exciton diffusion length (normally <20 nm).⁶ Prototype BHJ cells consist of an n-type [6,6]-phenyl C61-butyric acid methyl ester (PCBM) and a p-type conjugated organic polymer which form bicontinuous interpenetrating phase structures with the blend films.^{1e} In contrast, solar cells based on small molecules did not receive much attention until recently.⁷ Up to 3.4% and 5.0% efficiencies for vacuum-deposited layered OPV cells based on small molecules were reported by Pfeiffer⁸ and Forrest's⁹ groups, respectively. A high efficiency of 4.4% for a solution-processed BHJ solar cell was also demonstrated by Nguyen.^{7j} It is optimistic that solution-processable BHJ solar cells based on small molecules will have efficiencies higher than 5% in future.

In this paper, we report small molecules which have an electron-deficient dibenzo[*f,h*]thieno[3,4-*b*]quinoxaline entity with two peripheral arylamine units. The molecules may have several advantages: (1) dipolar characteristic due to charge transfer from arylamine to quinoxaline may be beneficial to red shifting the electronic absorption band; (2) the arylamine units are capable of hole transport; (3) the nonlinear fashion between the donor and the acceptor may facilitate separation of the electron and the hole. Scheme 1 depicts the synthesis

Scheme 1. Synthesis of the Compounds **1** and **2**



of two dipolar compounds **1** and **2**. 2,5-Bis(4-*tert*-butylphenyl)thiophene-3,4-diamine underwent condensation reaction

with diketone in the presence of catalytic amount of *p*-toluenesulfonic acid to form intermediate **1b** or **2b**, which then underwent palladium-catalyzed Stille coupling reaction with 9,9-dihexyl-*N,N*-diphenyl-7-(5-(tributylstannyl)thiophen-2-yl)-9*H*-fluoren-2-amine¹⁰ to provide the desired products.

The absorption spectra of the dyes in CH₂Cl₂ are displayed in Figure 1, and the data are collected in Table 1. Both

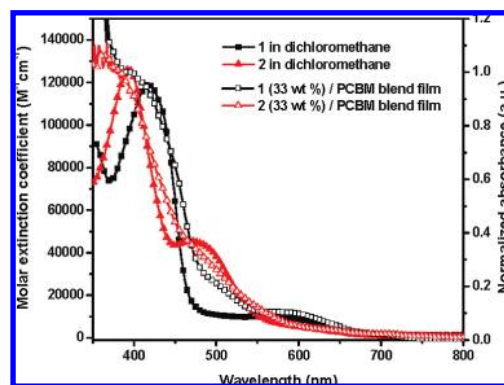


Figure 1. Absorption spectra of the dyes in dichloromethane. The normalized absorption spectra of **1** as a solution in CH₂Cl₂ and as a blend film coated from CHCl₃ solution.

compounds exhibit two distinct absorption bands: the one with very high molar extinction coefficient ($\sim 1.2 \times 10^5 \text{ M}^{-1} \text{ cm}^{-1}$) can be attributed to the $\pi-\pi^*$ transition of the thienquinoxaline core, and the weaker broad band at 580 nm (**1**) or 478 nm (**2**) is due to charge transfer from the arylamine to the quinoxaline. The charge transfer band of **2** exhibits hypsochromical shifts compared to **1**. This is consistent with theoretical computation results using density functional theory (DFT) at a B3LYP/6-31G* level of theory. The results for the theoretical approach are summarized in Table S1 (Supporting Information), and Figures S1 and S2 show selected frontier orbitals and calculated electronic

(6) Brabec, C. J.; Sariciftci, N. S.; Hummelen, J. C. *Adv. Funct. Mater.* **2001**, *11*, 15.

(7) (a) de Bettignies, R.; Nicolas, Y.; Blanchard, P.; Levillain, E.; Nunzi, J.-M.; Roncali, J. *Adv. Mater.* **2003**, *15*, 1939. (b) Cravino, A.; Leriche, P.; Al'vqñ, O.; Roquet, S.; Roncali, J. *Adv. Mater.* **2006**, *18*, 3033. (c) Lloyd, M. T.; Mayer, A. C.; Subramanian, S.; Mourey, D. A.; Herman, D. J.; Bapat, A. V.; Anthony, J. E.; Malliaras, G. G. *J. Am. Chem. Soc.* **2007**, *129*, 9144. (d) Tamayo, A. B.; Walker, B.; Nguyen, T.-Q. *J. Phys. Chem. C* **2008**, *112*, 11545. (e) Lincker, F.; Delbosc, N.; Bailly, S.; De Bettignies, R.; Billon, M.; Pron, A.; Demadrille, R. *Adv. Funct. Mater.* **2008**, *18*, 3444. (f) Silvestri, F.; Irwin, M. D.; Beberina, L.; Facchetti, A.; Pagani, G. A.; Marks, T. J. *J. Am. Chem. Soc.* **2008**, *130*, 17640. (g) Kronenberg, N. M.; Deppisch, M.; Würthner, F.; Lademann, K. D.; Meerholz, K. *Chem. Commun.* **2008**, 6489. (h) Rousseau, T.; Cravino, A.; Bura, T.; Ulrich, G.; Ziessel, R.; Roncali, J. *Chem. Commun.* **2009**, 1673. (i) Marrocchi, A.; Silvestri, F.; Seri, M.; Facchetti, A.; Taticchi, A.; Marks, T. J. *Chem. Commun.* **2009**, 1380. (j) Walker, B.; Tamayo, A. B.; Dang, X. D.; Jung, P. Z.; Seo, H.; Garcia, A.; Tantiawat, M.; Nguyen, T. Q. *Adv. Funct. Mater.* DOI: 10/1002/adfm.200900832. (k) Wong, W. W. H.; Jones, D. J.; Yan, C.; Watkins, S. E.; King, S.; Haque, S. A.; Wen, X.; Ghiggino, K. P.; Holmes, A. B. *Org. Lett.* **2009**, *11*, 975.

(8) Schllze, K.; Uhrich, C.; Schüppel, R.; Leo, K.; Pfeiffer, M.; Brier, E.; Reinold, E.; Buerle, P. *Adv. Mater.* **2006**, *18*, 2872.

(9) Xue, J.; Rand, B. P.; Uchida, S.; Forrest, S. R. *Adv. Mater.* **2005**, *17*, 66.

(10) Stille, J. K. *Angew. Chem., Int. Ed.* **1986**, *25*, 508.

Table 1. Electrooptical Parameters of the Dyes^a

dye	λ_{max} , nm ($\epsilon \times 10^{-4} \text{ M}^{-1} \text{ cm}^{-1}$)	E_{ox} (mV)	E_{red} (mV)	HOMO (eV)	LUMO (eV)
1	580 (0.97), 417 (11.9), 352 (9.20), 317 (8.57)	368, 601, 820	−1484	−5.16	−3.34
2	478 (4.47), 393 (12.6), 314 (6.40)	369, 537, 831	−1486	−5.16	−2.93

^a Absorption and electrochemical data were collected in CH₂Cl₂ solutions. Potentials are quoted with reference to the internal ferrocene standard ($E_{1/2} = +256 \text{ mV}$ vs Ag/AgNO₃).

transitions (Supporting Information), respectively. The higher energy band for **1** stems from $S_0 \rightarrow S_5$, whereas that of **2** is higher in energy and consists mainly of $S_0 \rightarrow S_6$ and $S_0 \rightarrow S_7$. This band indeed has strong $\pi-\pi^*$ transition character. The lower energy bands for both **1** and **2** have prominent charge-transfer character. In **1**, this band mainly stems from the $S_0 \rightarrow S_1$ transition. In comparison, the same band with much higher intensity in **2** consists of $S_0 \rightarrow S_2$ and $S_0 \rightarrow S_3$ transitions where charge transfer dominates. The same trend was also observed for isomeric 2,7-bis(9',9'-dioctyl)fluoren-2'-yl)-9,10-phenanthraquinone and 3,6-bis(9',9'-dioctyl)fluoren-2'-yl)-9,10-phenanthraquinone.¹¹ The absorption spectrum of the compounds as a film on ITO glass is very similar to that in the solution except that the band is somewhat broadened in the longer wavelength region (Figure 1), suggesting the presence of J-aggregation of the molecules in the film state.

The electrochemical data of the compounds are listed in Table 1, and the cyclic voltammograms are shown in Figure S3 (Supporting Information). Similar to our previous observations on bipolar compounds with a benzo[1,2,5]thiadiazole core and two peripheral diarylamines,¹² the oxidation of the peripheral amines was detected as a quasireversible two-electron redox wave, indicating no significant interaction between the two amines. The redox waves at higher potentials may be due to the oxidation of dibenzo[*f,h*]-thieno[3,4-*b*]quinoxaline core and the oxidation of thienylfluorene segment, respectively. A one-electron wave at −1.48 V is attributed to the reduction of dibenzo[*f,h*]-thieno[3,4-*b*]quinoxaline core. The HOMO energy level of **1** was calculated to be −5.16 eV from cyclic voltammetry by comparison with ferrocene (4.8 eV).¹³ This together with the HOMO/LUMO gap (**1**: 1.82 eV; **2**, 2.23 eV) calculated from the absorption band edge were used to obtain the LUMO energy level (**1**: −3.34 eV; **2**, −2.93 eV). Based on the relative HOMO and LUMO energy levels of the compounds and PCBM (HOMO = −4.1; LUMO = −6.1 eV; Figure S4, Supporting Information), it is appropriate to use them and PCBM in OPV cells as p- and n-type materials, respectively.

BHJ cells with a **1**/PCBM blend in a 1:1 weight ratio as the active layer were fabricated by spin coating on a PEDOT/PSS/ITO substrate (PEDOT/PSS = poly(3,4-ethylenedioxythiophene)/poly(styrenesulfonate)). PEDOT/PSS was used to

facilitate hole injection from the organic layer to ITO anode and to alleviate the surface roughness of ITO. Chloroform, chlorobenzene, and *o*-dichlorobenzene were chosen first to cast the active layers. The performance parameters of the cells are listed in Table 2. The photovoltage in each cell

Table 2. Device Parameters with Films Spin-Coated from 1:1 Weight Ratio of **1**/PCBM Dissolved in Different Solvents

solvent	V_{oc} (V)	J_{sc} (mA cm ^{−2})	η (%)	FF
chlorobenzene	0.87	2.00	0.55	0.32
<i>o</i> -dichlorobenzene	0.87	2.33	0.60	0.30
chloroform	0.90	2.60	0.75	0.32

reached ~0.9 V, close to the ideal value estimated from the difference between the HOMO level of **1** and LUMO level of PCBM. Moreover, the BHJ cell made from chloroform has a rather high conversion efficiency as well as photocurrent. In viewing that the cell fabricated from chloroform has the best performance among the three solvents used, BHJ cells with three different weight ratios of **1**/PCBM were also fabricated from the blends in chloroform. The *J*–*V* curves from different cells with postannealing of the blend films are shown in Figure S5 (Supporting Information), and the corresponding parameters are collected in Table 3. The cell with a 67 wt % of PCBM had optimal efficiency at 1.70%. The external quantum efficiency (EQE) in the region 350–600 nm surpassed that of the BHJ cell based on pristine P3HT/PCBM (P3HT = poly(3-hexylthiophene)).¹⁴ In the region 373–440 nm, the EQE is above 55%, which surpasses that observed in the BHJ cell based on annealed P3HT/PCBM.¹⁴ However, the EQE value is lower compared to the annealed cell of P3HT/PCBM at longer wavelengths. BHJ cells of **2** with PCBM at 50, 67, and 80 wt % were also checked. The cell with a 67 wt % of PCBM exhibited the best conversion efficiency. Though the cell had comparable open-circuit voltage with that of the **1**-based cell, the significant drop in short-circuit resulted in a lower efficiency at 0.90% which was ~50% lower compared to the cell based on **1** with the same wt % of PCBM. The decreased efficiency is mainly due to the drop of short-circuit current in the cell of **2**. It is possible that there is inferior film morphology and/or imbalanced carrier mobility for the film of **2**.

The electron and hole mobilities for **1**/PCBM film were computed by analyzing their dark *J*–*V* curves which are

(11) Gautrot, J. E.; Hodge, P.; Helliwell, M.; Raftery, J.; Cupertino, D. *J. Mater. Chem.* **2009**, *19*, 4148.

(12) Justin Thomas, K. R.; Lin, J. T.; Velusamy, M.; Tao, Y.-T.; Chuen, C.-H. *Adv. Funct. Mater.* **2004**, *14*, 83.

(13) (a) Pommerehne, H.; Vestweber, H.; Guss, W.; Mahrt, R. F.; Bässler, H.; Porsch, M.; Daub, J. *Adv. Mater.* **1995**, *7*, 551. (b) Thelakkat, M.; Schmidt, H. *Adv. Mater.* **1998**, *10*, 219.

(14) Yang, X.; Loos, J.; Veenstra, S. C.; Verhees, J. H.; Wienk, M. M.; Kroon, J. M.; Michels, M. A. J.; Janssen, A. J. *Nano. Lett.* **2005**, *5*, 579.

Table 3. Summary of Device Parameters at Various 1/PCBM and 2/PCBM Compositions

sample	μ_e ($\text{m}^2 \text{V}^{-1} \text{s}^{-1}$)	μ_h ($\text{m}^2 \text{V}^{-1} \text{s}^{-1}$)	V_{OC} (V)	J_{SC} (mA cm^{-2})	FF	η (%)
1/PCBM 50 wt %	1.61×10^{-8}	3.14×10^{-8}	0.90	2.60	0.32	0.75
1/PCBM 67 wt %	2.94×10^{-8}	1.95×10^{-8}	0.89	4.15	0.46	1.70
1/PCBM 80 wt %	6.90×10^{-8}	5.42×10^{-9}	0.74	2.13	0.30	0.48
2/PCBM 50 wt %			0.91	2.36	0.33	0.70
2/PCBM 67 wt %			0.92	2.87	0.34	0.90
2/PCBM 80 wt %			0.91	2.49	0.34	0.77

related by a relation $J = 9\varepsilon_0\varepsilon_r\mu V^2/8L^3$ where $\varepsilon_0\varepsilon_r$ is the dielectric permittivity of the polymer, μ is the carrier mobility, and L denotes the thickness of the active layer.¹⁵ The relevant data are collected in Table 3. Balanced electron and hole mobility are beneficial to the device performance; the one with the highest efficiency (67 wt % PCBM) has the ratio of electron/hole mobility (μ_e/μ_h) at ~ 1.5 and the one with the poorest efficiency has electron/hole mobility at ~ 13 . It is also worth noting that the system with more balanced charge transport had higher current density value. The morphologies of the active layers with different weight ratios of PCBM/1 were also investigated by atomic force microscopy (AFM, Digital instrument NS 3a controller with D3100 stage). The AFM images of these films are shown in Figure S6 (Supporting Information). The blends formed smooth films, and the root-mean-square (rms) roughness was smaller than 3 nm. Film morphology was further examined by transmission electron microscopy (TEM), and the TEM micrograms of the annealed blend films¹⁶ of 1/67 wt % of PCBM and 1/80 wt % of PCBM are shown in Figure 2. Though no resolvable interpenetrating network frequently

observed in blend film of polymer/PCBM¹⁶ can be detected, it is evident that the film of 1/67 wt % PCBM has smoother morphology than that of 1/80 wt % PCBM. This gives further support for the better performance of BHJ cell from 1/67 wt % PCBM.

In conclusion, new bipolar compounds containing dibenzo[*f,h*]thieno[3,4-*b*]quinoxaline and arylamine motifs were synthesized and characterized. Besides intense $\pi-\pi^*$ transition, the charge-transfer transition in these compounds also contributes to light harvesting. Because of good solubility of the compound in common organic solvents, solution-processable BHJ cells with good power conversion efficiencies can be achieved from the blends of the compound and PCBM. The performance of the cells depends on the solvent used for fabrication and the ratio of the compound vs PCBM. The cell fabricated from a CHCl_3 blend of one of the compounds with 67 wt % of PCBM has the best performance, with the conversion efficiency reaching 1.70% and high EQE values close to 60% in the 380–420 nm region. Further improvement of the device efficiency by tuning of the molecular structure as well as device fabrication is currently under investigation.

Acknowledgment. We would like to acknowledge the Academia Sinica, National Taiwan University, and National Science Council, Taiwan, for financial support. We thank the Cryo-EM Common Facility of Scientific Instrument Center, Academia Sinica, for TEM service.

Supporting Information Available: Synthetic procedures and characterization for new compounds. This materials is available free of charge via the Internet at <http://pubs.acs.org>.

OL9019953

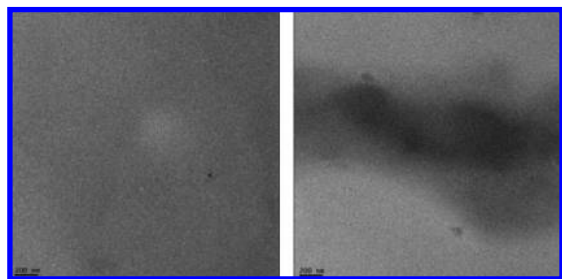


Figure 2. TEM images for the annealed blend films of 1/67 wt % PCBM and 1/80 wt % PCBM. The scale bars in both images are 200 nm.

(15) Hertel, D. H.; Bässler, H. *ChemPhysChem* **2008**, 9, 666.

(16) The films were prepared following the procedures reported in the following paper: Sivula, K.; Luscombi, C. K.; Thompson, B. C.; Fréchet, J. M. J. *J. Am. Chem. Soc.* **2006**, 128, 13988.